ESTEEM Academic Journal
Vol. 16, December 2020, 65- 74

Computational Analysis of Fluid Flow Past a Bluff Body at Low Reynolds Number in Different Apex Angle

Jusoh, M.Z.M.[1], Nur Ain, A.R[2] and Muhammad Wafi Md Nor[3]
Faculty of Mechanical Engineering, Universiti Teknologi MARA, Cawangan Terengganu, Kampus Bukit Besi Malaysia
**corresponding author: [1]zaminmj@uitm.edu.my*

ARTICLE HISTORY

Received
14 October 2020

Accepted
29 November 2020

Available online
30 December 2020

ABSTRACT

A computational fluid dynamic analysis (CFD) is presented in the study of low Reynolds number fluid flow moving past bluff bodies. The study is focusing on the understanding of the effects of the apex-angles orientation on the flow structure and related occurring force. The apex-angle both facing upstream and downstream were computationally investigated. The simulation results of the cylinder solid are compared with available experimental data to justify the results and the model used. Results obtained in the present work were Strouhal number, drag coefficient, and Fast Fourier Transform (FFT). The study had found that the value of the drag force is increasing directly proportional to the apex angle. In contrast, the value of Strouhal number inversely proportional to the increasing of the apex angle. This was due to the flow over a cylinder creating a vortex shedding in the wake region which influenced the flow separation of fluid. Through the changing on orientation of the apex angle, it was also found that the characteristic linear dimension of the geometry will also be changed, thus affecting the flow pattern.

Keywords: *apex angle; laminar; transient; triangular; bluff body.*

1. INTRODUCTION

Characteristics of fluid flow around bluff bodies have become a focus of researchers' investigation because of their importance in various engineering applications [1]. Flow over a cylinder is an example of a fundamental fluid mechanics problem in which the pattern of this flow varies depending upon the Reynolds number, [2]. The flow field over the cylinder is symmetric at a low Reynolds number. As the Reynolds number increases, flow begins to separate behind the cylinder causing vortex shedding [3]. Hence, Oliveira [4] also observed that the drag forces acting on the cylinder walls correspond to the increasing Reynolds number. Lehmkuhl [5] stated that for the triangle prism or cylinder, as the Reynolds number increases up to the critical Reynolds number, flow is still symmetric, but eddies are formed, and the symmetric flow region decreases and changes to an asymmetric area. The Reynolds number is the ratio of inertia force to viscous force, which can be written as Equation 1:

$$Re = \frac{Inertial\ force}{Viscous\ force} = \frac{VD}{v} = \frac{\rho VD}{\mu} \quad (1)$$

where V is the average flow velocity, D is the diameter of the cylinder (characteristic length), v is the kinematic viscosity, μ is the dynamic viscosity, and ρ, is the density of the fluid.

p-ISSN 1675-7939; e-ISSN 2289-4934

Vortex shedding is an oscillating flow when a fluid such as air or water flows past over a bluff body at specific velocities, depending on the body size and shape [6]. Bai [7] had found that the frequency of vortex shedding depends on the wake width, which is a function of whether the wake is formed by a shear layer separating from a downstream or an upstream corner. At Reynolds numbers beyond ReCritical, the unsteady flow develops several visually different vortex streets [8]. Srikanth [9] had investigated that the critical Reynolds number for the stationary triangular cylinder facing upstream is between 35 and 38.3. The wake is expected to be much broader through the previous studies on the triangular cylinder compared to the circular cylinder. As the most significant side of the triangular cylinder is up-stream, it is noted that the sheds created powerful vortices [10]. The vortex formation at the back of the cylinder depends on many parameters such as characteristic length, L, and angle of incidence, α [11].

In the literature, the studies about flow past a triangular cylinder are rarely investigated and discovered by the researcher. Thus, the present study aims to add and validate the existing knowledge of fluid flow over a triangular prism and cylinder through the computational simulation (ANSYS) approach. Furthermore, detailed information regarding the flow field for this triangular geometry is missing. Flow past a triangular cylinder can be varied by modifying the apex angles, angle of incidences, and characteristic length. A computational study of fluid flow around the triangular prism and cylinder bluff bodies is yet to be conducted/ has been conducted?. The focus of this study is towards the understanding of the effects of the orientation of the apex angles on the flow structure and related occurring force. The apex-angle both facing upstream and downstream were computationally investigated. The cylinder solid's simulation results are compared with available experimental data to justify the results and the model used. Results obtained in the present work were Strouhal number, drag coefficient, and Fast Fourier Transform (FFT) by transient simulation with the viscous-laminar model of ANSYS-Fluent software. The flow over a cylinder creates a vortex shedding in the wake region of bluff bodies because of the unsteady flow separation of fluid; this phenomenon is well-known as Von Karman Street. The characteristic linear dimension (L) of the geometry will also be changed through the changing or orientation of the apex angle, thus affecting the flow pattern.

2. DETAILS OF THE CFD SIMULATION PROCESS

2.1. Modelling

The flow field around the cylinder is modelled in two dimensions with the cylinder's axis perpendicular to the direction of flow. The cylinder is modeled as circular and triangular with a scale length of 1 m perpendicular towards the streamflow, and then a square flow domain is created around the cylinder [12]. Models used in the present study were five isosceles triangular cylinders with different apex angles of 15º, 30º, 45º, 60º, and 75º, both facing upstream and downstream as shown in figure 2 (a) and 2 (b). An increment of 15° had been used as a limitation to the study to observe the fluid behavior on a rotating cylinder. The 2-Dimensional geometry of the cylinder and the fluid domain were drawn by using ANSYS-Design-modeller. The cylinder obstacle is in the middle of the domain and at an upstream distance of X_a =12L from the inlet and at a downstream distance of X_b = 20L from the outlet while the upper and bottom wall distance of Y_a = 20L, where L is the scale length of the cylinder as shown in figure 2 (c). These values are chosen to reduce the effects of boundaries and satisfy the free stream condition consistent with other studies in the literature [13]. The 2-Dimensional Unstructured

p-ISSN 1675-7939; e-ISSN 2289-4934

triangles mesh was generated using Ansys-Meshing for both models to compute the flow around the model, as shown in figure 2 (d) and figure 2 (e).

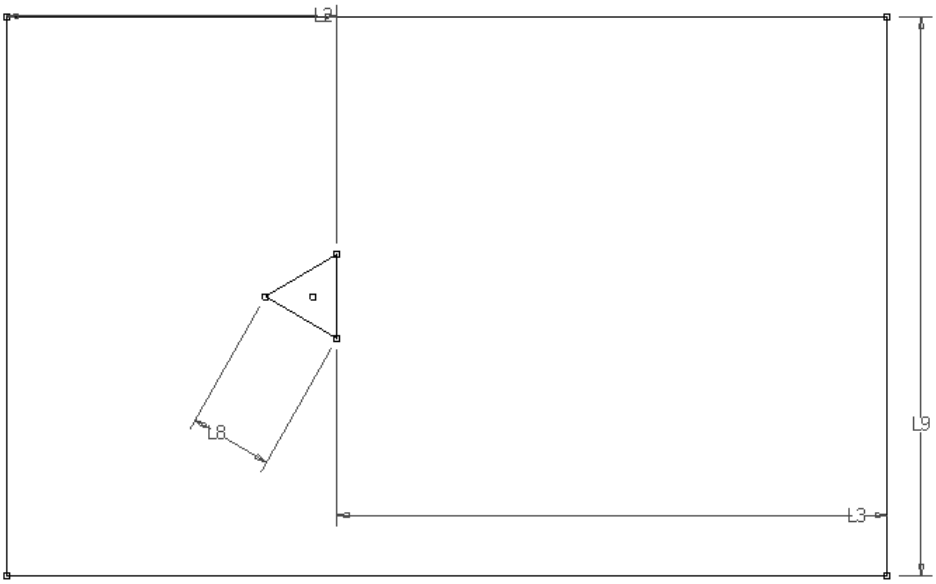

Figure 2(a): Schematic diagram of fluid domain for triangular cylinder with apex angle facing upstream

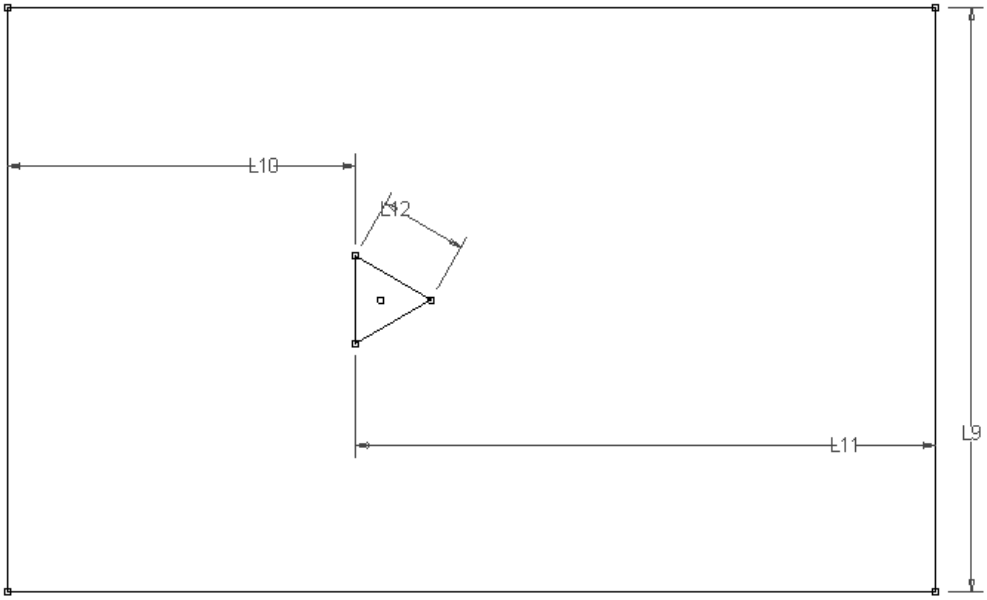

Figure 2 (b): Schematic diagram of fluid domain for triangular cylinder with apex angle facing downstream

p-ISSN 1675-7939; e-ISSN 2289-4934

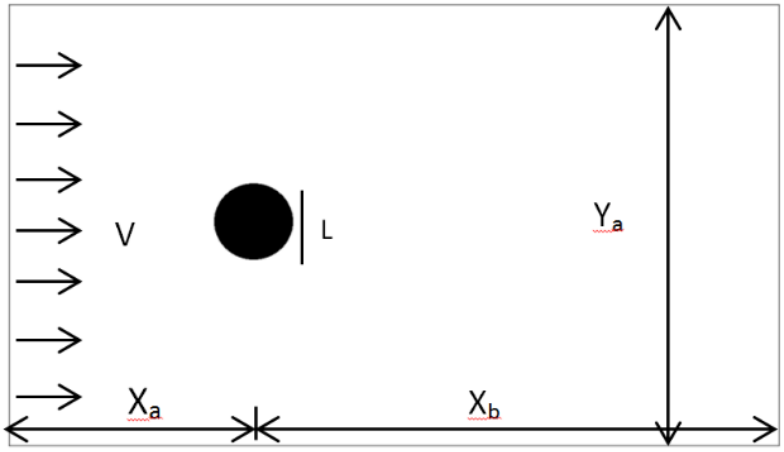

Figure 2(c): Schematic diagram of the 2-D model

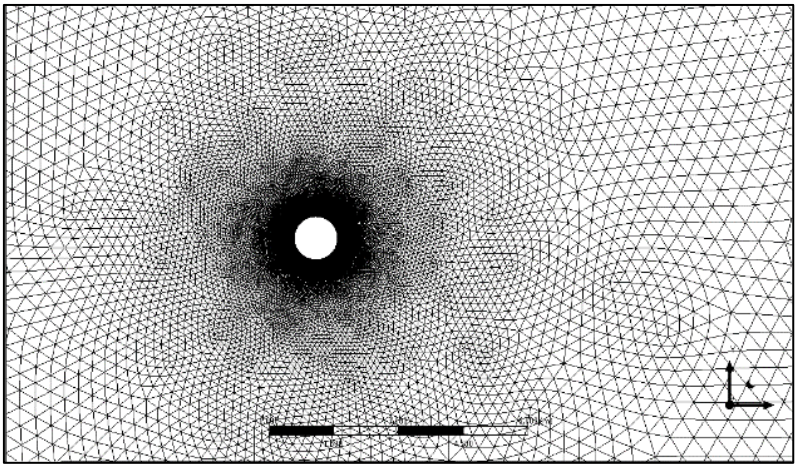

Figure 2(d): Cut-cell grid system around a circular cylinder

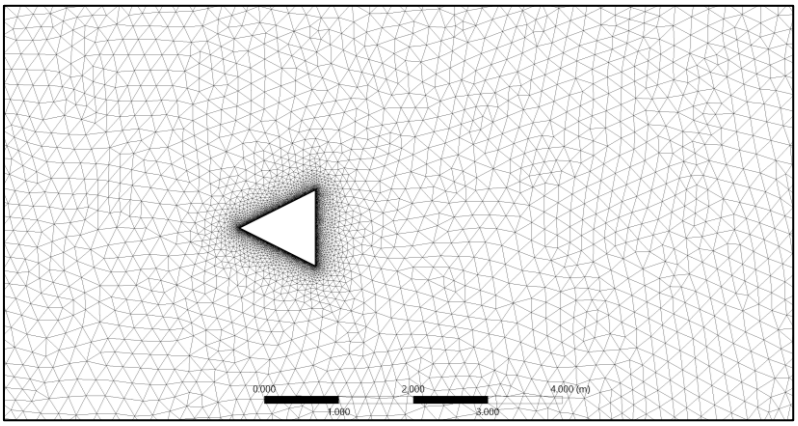

Figure 2(e): Cut-cell grid system around a triangular cylinder

p-ISSN 1675-7939; e-ISSN 2289-4934

2.2. Grid refinement

To ensure the dynamics flow is captured with sufficient accuracy, the grid refinement study is conducted by increasing the node and element in circular cylinder mesh. The mesh selected for monitoring the Strouhal number St, lift force coefficient, C_L, drag force coefficient C_D, and vorticity. Then the same mesh setup was used in conducting the triangular prism analysis to obtain the dynamic flow. Table 1 summarizes the grid refinement study.

Table 1: Grid refinement study

Mesh	**Circular**			**Triangular**
	Node Size	C_d	St	Nodes
Coarse	$12x10^3$	1.2935	0.109	$11x10^3$
Medium	$30x10^3$	1.3132	0.115	$25x10^3$
Fine	$50x10^3$	1.3024	0.115	$46x10^3$

2.3. Solver

The 2-Dimensional numerical simulation by the solver was made after the completion of the mesh generation. The solver formulation, transient viscous laminar model, boundary condition (BC), solution control parameters, and material properties were defined as shown in Table 2.

Table 2: Boundary condition setup

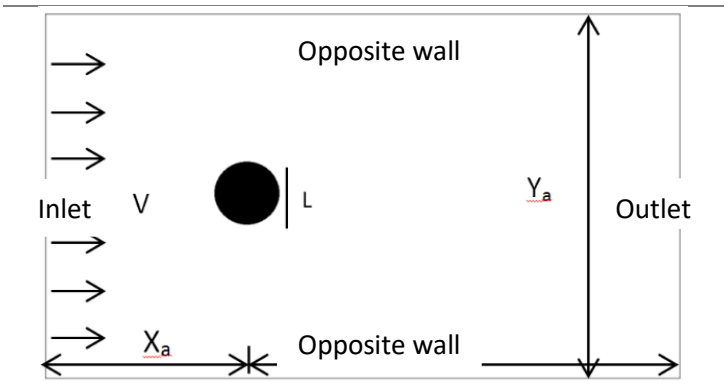

BC	Setup
Inlet	Velocity inlet
Outlet	Pressure outlet
Cylinder and opposite wall	Wall (non-slip)

After all the parameters were specified, the model was initialized. The initializing and iteration processes stopped after the completion of the computations. The results of instantaneous velocity, pressure, and dynamics flow obtained were examined and analyzed. The periodic graph of the lift coefficient is used to determine the Strouhal number.

3. RESULT AND DISCUSSION

The result of the 2-Dimensional triangular cylinder was compared to the 2-Dimensional circular cylinder. The discussions were focused on the aerodynamic characteristics, which include drag

p-ISSN 1675-7939; e-ISSN 2289-4934

coefficient C_D and Strouhal number, *St*. The drag coefficient, C_D is an important characteristic in measuring the resistance of the cylinder body. Eq 2 show the relationship between the fluid flow properties and the drag force:

$$C_D = \frac{2F_D}{\rho V^2 A} \tag{2}$$

where F_D is the drag force, ρ is the fluid density, V is the velocity of the fluid relative to the particle, and A is the projected cross-sectional area. Hence, Strouhal number,*St* is describe as ratio of inertial forces due to the local acceleration of the flow to the inertial forces due to the convective acceleration. The Strouhalnumber is a dimensionless number to represent the oscillating flow mechanisms which the equation is written as follows:

$$S_t = \frac{\omega L}{U} \tag{3}$$

where ω is the vortex shedding frequency, L is the characteristic length, and U is the free-stream velocity. In addition, the pressure and velocity contours, vector velocity, streamline, and vorticity will also be observed and studied. The simulation was carried out at various apex angles between 15° and 75° with an apex angle facing upstream and downstream. The simulation was done for flow past triangular prism at Reynolds number of Re=150 to observe the flow separation and the vortex shedding behind the cylinder wake.

Table 3: Drag coefficient and Strouhal number of both triangles facing upstream and downstream

Apex Angle, θ (°)	**Apex Angle Facing Upstream**		**Apex Angle Facing Downstream**	
	Strouhal Number, *St*	Drag Coefficient, C_D	Strouhal Number, *St*	Drag Coefficient, C_D
15	0.627	0.281	0.516	0.317
30	0.383	0.688	0.167	0.813
45	0.151	1.145	0.094	1.443
60	0.094	1.809	0.069	2.222
75	0.108	2.299	0.091	3.038

3.1. Drag Coefficient and Strouhal Number analysis

Figure 3(a) shows the drag coefficient, C_D changes with apex angle, ɵ for triangle both facing upstream and downstream. The data shows a definite trend in total drag coefficient with the increase in apex angle for both triangles with the apex angle facing upstream and downstream [14]. A quick comparison for both triangles of 75° apex angle facing upstream and downstream indicates the highest drag coefficient while the 15° triangle has the lowest drag coefficient [15]. The shape or geometry has a significant effect on the amount of drag produced. As can be seen in Table 3, the closest drag coefficient with a circular cylinder from Table 1 (C_D=1.302) is 45° triangle prism facing (C_D=1.443). Since the circular cylinder, C_D has the closest value to the experiment data, and this shows that at the apex angle of 45°, the flow around the triangular prism behaves similarly with the circular cylinder.

p-ISSN 1675-7939; e-ISSN 2289-4934

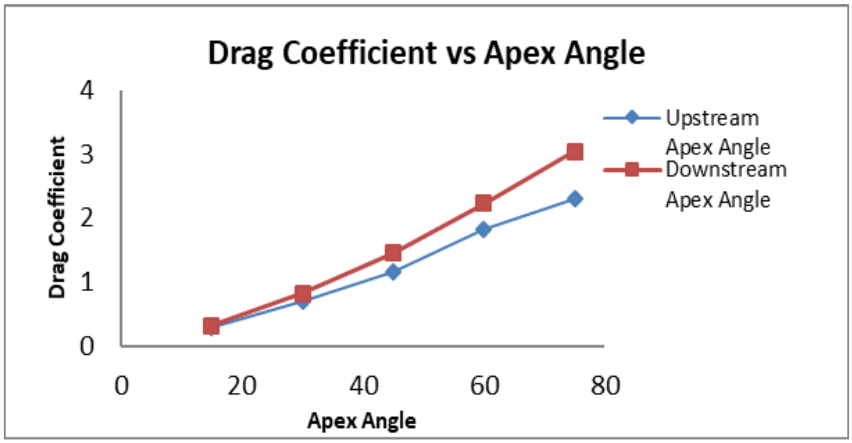

Figure 3(a): Drag Coefficient, C_D versus apex angle, ɵ

As evidenced in the figure above, with the increase in apex angle, the cylinder becomes bluffer and increases the drag coefficient, C_D. The value of C_D is increasing directly proportional to the wake size occuring behind the bluff body, as shown in Table 4. From table 4, at minimal characteristic length, L, a stable pair of vortices is formed on the downstream side. Therefore, as the characteristic length, L, increases, the vortices become unstable and are alternately shed downstream.

Figure 3(b) presents the Strouhal number, St changes with apex angle, ɵ for triangle both facing downstream and upstream. The graph indicates that the value of *St* inversely proportional to the apex angle for both upstream and downstream. It also found that the Strouhal number for a triangular at the apex angle 75° is *St= 0.108*, similar to the St value of the circular cylinder, *St = 0.111*, close to the experimental value. Figure 3(b) also shows the highest Strouhal number is at an apex angle 15º and a minimum at 75º. A higher Strouhal number is related to positive interaction between the different shear layers and better mixing of the flow and weakening of the wake. Table 4 shows that the dropping in Strouhal number is due to a sharp increase in the wake width as the flow separation on the triangular lateral face from the downstream corner to the upstream corner [16]

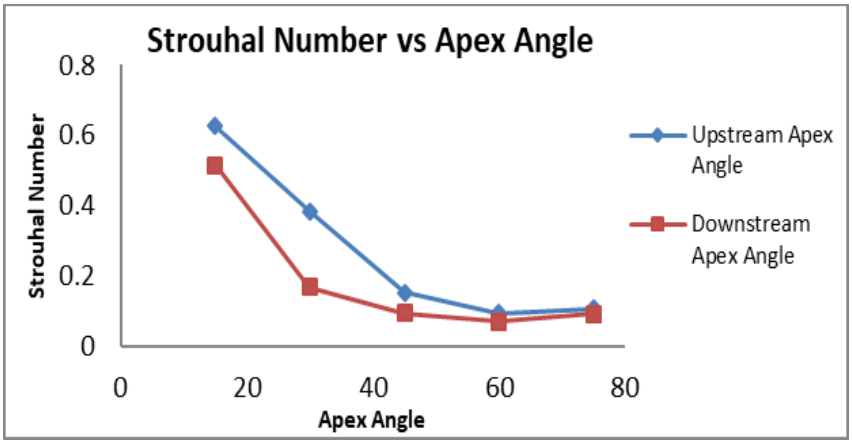

Figure 3(b): Strouhal Number, *St* versus apex angle, ɵ

.

p-ISSN 1675-7939; e-ISSN 2289-4934

3.2. Vorticity Contour and Fast Fourier Transform (FFT)

Table 4: Fast Fourier Transform for a triangular and circular cylinder

Cylinder	Vorticity Contour	Fast Fourier Transform (FFT)
Circular	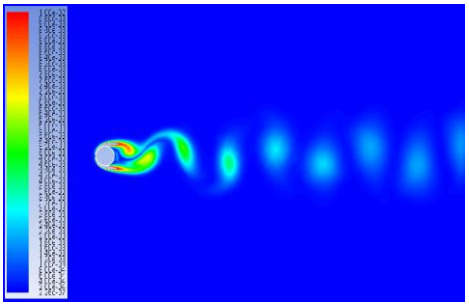	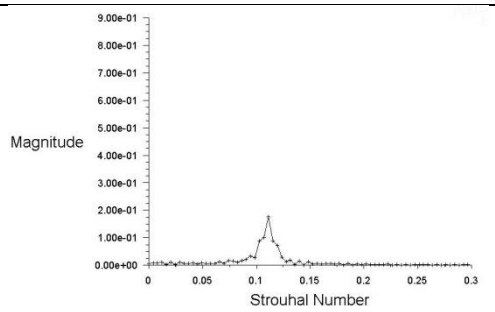
Apex Angle Facing upstream (15º)	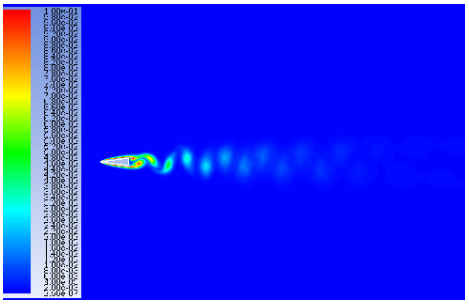	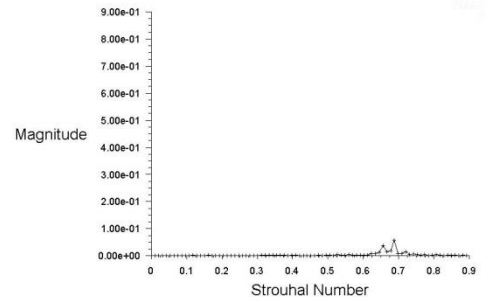
Apex Angle Facing upstream (75º)	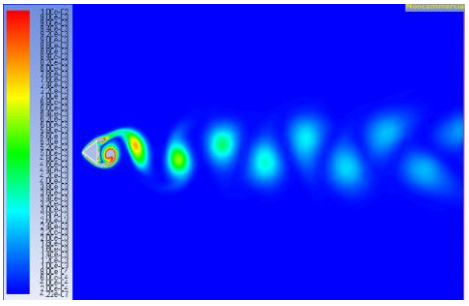	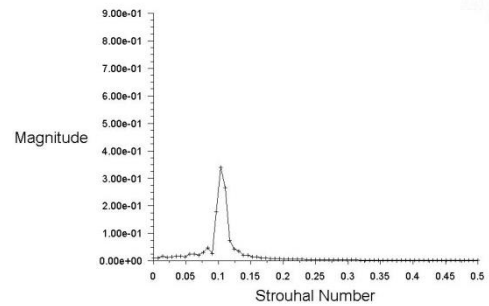
Apex Angle Facing Downstream (15º)	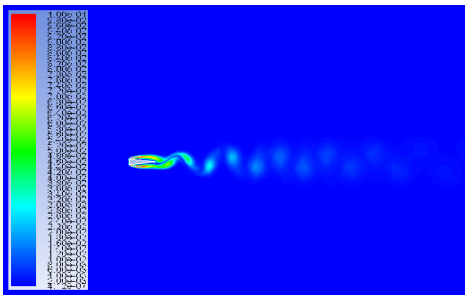	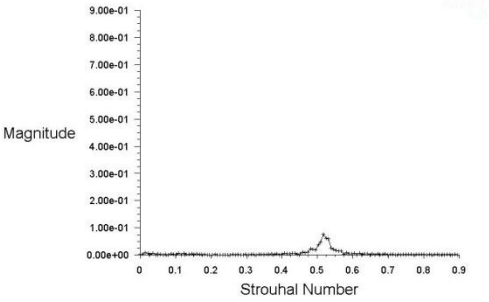
Apex Angle Facing Downstream (75º)	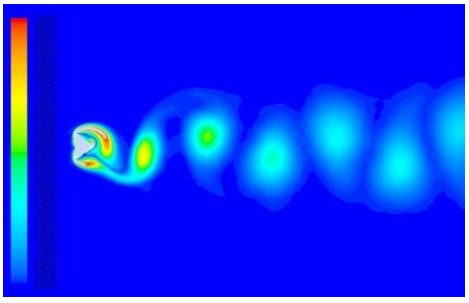	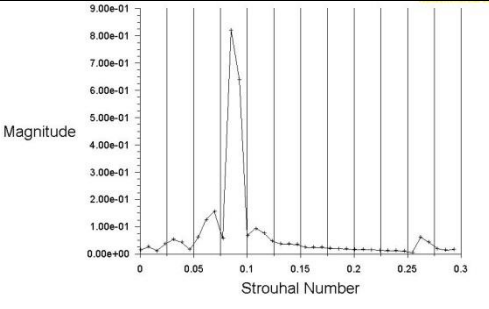

p-ISSN 1675-7939; e-ISSN 2289-4934

The figure in Table 4 presents the vorticity of a circular cylinder and triangular cylinder with 15^o and 75^o apex angle both facing up-stream and downstream. A clear vortex street is found for all cylinders, including circular and triangular. This shed roll-up is the vortex that moves further downstream. This alternate vortex shedding forms the Karman vortex street that is visible in visual. A quick comparison from the figure above discovers that the most intense flow structures formed are in the wake region behind the 75^o prism for both upstream and downstream flow. The small recirculation zone is observed for a triangle with an apex angle of 15^o. Even though the circular cylinder develops an intense vortex shedding, the circular cylinder magnitude has a lower value compared to 75° triangles as seen in Fast Fourier Transform (FFT) [17]. Therefore, the higher the magnitude, the intense the vortex shed will develop. The size of this turbulence contour is observed to increase with an average of 0.5 m with the increment in apex angle. In contrast, the Strouhal number is found to decrease with an increase in the apex angle. There is a delay in vortex shedding as the large vortices required a longer time to form. As a result, smaller vortices mean higher vortex shedding frequency and vice versa.

4. CONCLUSION

Laminar viscous flow over a triangular prism with apex angle both facing upstream and downstream is investigated by an ANSYS Fluent simulation. Different ranges of the apex angle in the laminar regime with Reynolds number of Re = 150 are investigated. Streamlines and flow parameters like drag coefficient are investigated. Drag coefficients on the triangular cylinder increase with the increase of the apex angle for both upstream and downstream. While for the flow visualization it shows that the wake increases with the increasing of apex angle and are in qualitative agreement with corresponding data reported in the literature for both apex angles facing upstream and downstream.

REFERENCES

[1] M. I. Yuce and D. A. Kareem, "A numerical analysis of fluid flow around circular and square cylinders," *J. Am. Water Works Assoc.*, vol. 108, no. 10, pp. E546–E554, 2016.

[2] T. Sato, Masami, Kobayashi, "A fundamental study of the flow past a circular cylinder using Abaqus/CFD," *2012 SIMULIA Community Conf.*, pp. 1–15, 2012.

[3] S. Ganga Prasath, M. Sudharsan, V. Vinodh Kumar, S. V. Diwakar, T. Sundararajan, and S. Tiwari, "Effects of aspect ratio and orientation on the wake characteristics of low Reynolds number flow over a triangular prism," *J. Fluids Struct.*, vol. 46, pp. 59–76, 2014.

[4] M. A. De Oliveira, P. G. De Moraes, C. L. De Andrade, A. M. Bimbato, and L. A. A. Pereira, "Control and suppression of vortex shedding from a slightly rough circular cylinder by a discrete vortex method," *Energies*, vol. 13, no. 17, 2020.

[5] O. Lehmkuhl, I. Rodríguez, R. Borrell, J. Chiva, and A. Oliva, "Unsteady forces on a circular cylinder at critical Reynolds numbers," *Phys. Fluids*, vol. 26, no. 12, 2014.

[6] G. Schewe, "Reynolds-number effects in flow around more-or-less bluff bodies," *J. Wind Eng. Ind. Aerodyn.*, vol. 89, no. 14–15, pp. 1267–1289, 2001.

[7] H. Bai and M. M. Alam, "Dependence of square cylinder wake on Reynolds number," *Phys. Fluids*, vol. 30, no. 1, 2018.

[8] Z. Y. Ng, T. Vo, W. K. Hussam, and G. J. Sheard, "Two-dimensional wake dynamics behind cylinders with triangular cross-section under incidence angle variation," *J. Fluids Struct.*, vol. 63, pp. 302–324, 2016.

[9] Z. Ng, W. Hussam, and G. Sheard, "Wake Structures of Unsteady Two-Dimensional Flows Past Cylinders With Triangular Cross-Sections," *11th Int. Conf. CFD Miner. Process Ind.*, no. December, pp. 1–6, 2015.

p-ISSN 1675-7939; e-ISSN 2289-4934

[10] S. Srikanth, A. K. Dhiman, and S. Bijjam, "Confined flow and heat transfer across a triangular cylinder in a channel," *Int. J. Therm. Sci.*, vol. 49, no. 11, pp. 2191–2200, 2010.
[11] J. Tu, D. Zhou, Y. Bao, Z. Han, and R. Li, "Flow characteristics and flow-induced forces of a stationary and rotating triangular cylinder with different incidence angles at low Reynolds numbers," *J. Fluids Struct.*, vol. 45, no. 800, pp. 107–123, 2014.
[12] S. Camarri, M. V. Salvetti, and G. Buresti, "Large-eddy simulation of the flow around a triangular prism with moderate aspect ratio," *J. Wind Eng. Ind. Aerodyn.*, vol. 94, no. 5, pp. 309–322, 2006.
[13] M. I. N. M. I. N. Htun, "A Study in Flow Past Triangular Cylinders With Different Apex Angles," *ScholarBank@NUS Repository*, 2004.
[14] S. Longo, A. Valiani, L. Lanza, and D. Liang, "Experimental study of the grain-water mixture flow past a cylinder of different shapes," *Eur. J. Mech. B/Fluids*, vol. 38, pp. 101–113, 2013.
[15] Z. Li and Z. Sun, "Development of the Vortex Mass Flowmeter with Wall Pressure Measurement," *Meas. Sci. Rev.*, vol. 13, no. 1, pp. 20–24, 2013.
[16] S. Oka and T. Ishihara, "Numerical study of aerodynamic characteristics of a square prism in a uniform flow," *J. Wind Eng. Ind. Aerodyn.*, vol. 97, no. 11–12, pp. 548–559, 2009.
[17] N. Agrwal, S. Dutta, and B. K. Gandhi, "Experimental investigation of flow field behind triangular prisms at intermediate Reynolds number with different apex angles," *Exp. Therm. Fluid Sci.*, vol. 72, pp. 97–111, 2016.

p-ISSN 1675-7939; e-ISSN 2289-4934